Recombinant endostatin forms amyloid fibrils that bind and are cytotoxic to murine neuroblastoma cells in vitro

Onno Kranenburg[a], Loes M.J. Kroon-Batenburg[b], Arie Reijerkerk[a], Ya-Ping Wu[c], Emile E. Voest[a], Martijn F.B.G. Gebbink[a,*]

[a] *Department of Medical Oncology, University Medical Center Utrecht, Heidelberglaan 100, 3584 CX Utrecht, The Netherlands*
[b] *Department of Crystal and Structural Chemistry, Bijvoet Center for Biomolecular Research, Utrecht University, Padualaan 8, 3584 CH Utrecht, The Netherlands*
[c] *Department of Haematology, University Medical Center Utrecht, Heidelberglaan 100, 3584 CX Utrecht, The Netherlands*

Received 9 February 2003; accepted 24 February 2003

First published online 6 March 2003

Edited by Gunnar von Heijne

Abstract **Endostatin is a fragment of collagen XVIII that acts as an endogenous inhibitor of tumor angiogenesis and tumor growth. Anti-tumor effects have been described using both soluble and insoluble recombinant endostatin. However, differences in endostatin structure are likely to cause differences in bioactivity. In the present study we have investigated the structure and cellular effects of insoluble endostatin. We found that insoluble endostatin shows all the hallmarks of amyloid aggregates. Firstly, it binds Congo red and shows the characteristic apple-green birefringe when examined under polarized light. Secondly, electron microscopy shows that endostatin forms short unbranched fibrils. Thirdly, X-ray analysis shows the abundant presence of cross-β sheets, the tertiary structure that underlies fibrillogenesis. None of these properties was observed when examining soluble endostatin. Soluble endostatin can be triggered to form cross-β sheets following denaturation, indicating that endostatin is a protein fragment with an inherent propensity to form amyloid deposits. Like β-amyloid, found in the brains of patients with Alzheimer's disease, amyloid endostatin binds to and is toxic to neuronal cells, whereas soluble endostatin has no effect on cell viability. Our results demonstrate a previously unrecognized functional difference between soluble and insoluble endostatin, only the latter acting as a cytotoxic amyloid substance.**

Key words: Endostatin; Amyloid; Aβ; IAPP; Aggregation; Cross-β; Neuron; Toxicity

1. Introduction

In recent years cancer therapy has seen the development of a new class of drugs: inhibitors of the formation of new blood vessels ('angiogenesis') which thereby limit blood supply to tumors. A number of anti-angiogenic compounds have proven to be effective in eradicating tumors in mouse models and are now being further tested in clinical trials (reviewed in [1–4]). Endostatin, a naturally occurring fragment of collagen XVIII, is considered to be one of the most effective inhibitors of angiogenesis [3]. Early studies with bacterially produced (insoluble) endostatin have shown its potent inhibitory effect on tumor growth [5,6]. Although soluble endostatin (produced in yeast) can also inhibit tumor growth, permanent tumor regression has only been reported when using insoluble endostatin [3]. Effects of endostatin on endothelial cell proliferation [5], apoptosis [7–9] and migration [10,11] have been described, but it is not clear to what extent these activities contribute to the anti-angiogenic and anti-tumor effects of endostatin in vivo. Moreover, it remains unclear why endostatin therapy works so well in some experiments [3] but remains ineffective in others [12–15] (and our own unpublished data). Different structural forms of endostatin are likely to have distinct bioactivities. Soluble and insoluble endostatin may therefore produce their anti-angiogenic effects through distinct mechanisms. In the present report we set out to investigate the structural and biological differences between soluble and insoluble endostatin. Whereas the structure of soluble, globular endostatin has been elucidated [16,17], the structure of insoluble endostatin has not. Insoluble proteins may occur as amorphous aggregates but they may also occur as highly ordered 'amyloid' deposits [18]. In the latter case, the polypeptide backbones are in a β-sheet conformation and are stacked through intermolecular (rather than intramolecular) hydrogen bonds, thus forming a 'cross-β sheet' [19]. We found that endostatin is a protein with high propensity to form amyloid fibers through extensive cross-β sheet formation. Fibrillar endostatin binds to neuronal cells and causes neuronal cell death, whereas soluble endostatin does not. Our results suggest that endostatin induces apoptosis as a result of its amyloid structure.

2. Materials and methods

2.1. Preparation of recombinant human endostatin from bacteria

Endostatin was purified from bacteria essentially as described in [6]. In short, Bl21.DE3 bacteria expressing endostatin were lysed in a buffer containing 8 M urea, 10 mM Tris (pH 8.0), 10 mM imidazole and 10 mM β-mercaptoethanol. Folllowing purification over Ni-agarose, the protein sample was extensively dialyzed against H_2O. During dialysis endostatin precipitates as a fine white solid. Aliquots of this material were either stored at −80°C for later use, or were freeze-dried prior to storage.

*Corresponding author. Fax: (31)-30-2523741.
E-mail address: m.gebbink@azu.nl (M.F.B.G. Gebbink).

Abbreviations: DMSO, dimethylsulfoxide; DMEM, Dulbecco's modified Eagle's medium; FITC, fluorescein isothiocyanate; PBS, phosphate-buffered saline; BSA, bovine serum albumin; Aβ, amyloid beta; hIAPP, human islet amyloid polypeptide; TEM, transmission electron microscopy

0014-5793/03/$22.00
doi:10.1016/S0014-5793(03)00218-7

2.2. Recombinant human endostatin from yeast

Endostatin produced by the yeast strain *Pichia pastoris* was kindly provided by Dr. Kim Lee Sim (EntreMed, Rockville, MA, USA).

2.3. Preparation of aggregated yeast-produced endostatin

Soluble yeast endostatin was dialyzed overnight in 8 M urea and subsequently three times against H_2O. Like bacterial endostatin, yeast endostatin precipitates as a fine white solid.

2.4. Amyloid β (Aβ) and human islet amyloid polypeptide (hIAPP)

$A\beta_{1-40}$ (DAEFRHDSGYEVHHQKLVFFAEDVGSNKGAIIGLMVGGVV) and hIAPP (KCNTATCATQRLANFLVHSSNNFGAILSSTNVGSNTY) were obtained from the peptide synthesis facility at the Netherlands Cancer Insitute (Amsterdam, The Netherlands). The freeze-dried peptides were resuspended in phosphate-buffered saline (PBS) and were allowed to form cross-β structure over a period of 3 weeks at room temperature. Cross-β sheet formation was followed by Congo red binding and examination of green birefringence under polarized light.

2.5. Congo red staining

Freeze-dried bacterial endostatin was resuspended in either 0.1% formic acid or in dimethylsulfoxide (DMSO) and taken up in a glass capillary. The solvent was allowed to evaporate and the resulting endostatin material was stained with Congo red (Sigma) according to the manufacturer's protocol.

2.6. Transmission electron microscopy (TEM)

Endostatin samples were applied to 400 mesh specimen grids covered with carbon-coated collodion films. After 5 min the drops were removed with filter paper and the preparations were stained with 1% methylcellulose and 1% uranyl acetate. After washing in H_2O the samples were dehydrated in a graded series of EtOH and hexamethyldisilazane. Transmission electron micrographs were recorded at 60 kV using a JEOL-1 electron microscope.

2.7. X-ray diffraction analysis

Aggregated endostatin was solubilized in 0.1% FA and was taken up in a glass capillary. The solvent was then allowed to evaporate over a period of several days. Capillaries containing the dried samples were placed on a Nonius κCCD diffractometer. Scattering was measured using sealed tube Mo Kα radiation with a graphite monochromator on the CCD area detector for a period of 16 h. Scattering from air and the glass capillary wall were subtracted using in-house software (VIEW/EVAL).

2.8. N1E-115 cell culture and differentiation

N1E-115 mouse neuroblastoma cells were routinely cultured in Dulbecco's modified Eagle's medium (DMEM) containing 5% fetal calf serum (FCS), supplemented with antibiotics. Cells were differentiated into post-mitotic neurons by culturing them in DMEM containing 0.5% FCS, 1 mM cAMP and 1% DMSO for 48 h.

2.9. Fluorescein isothiocyanate (FITC)-labeling and fluorescence microscopy

Soluble (yeast-produced) endostatin was dialyzed against 0.01 M $Na_2B_4O_7$–0.15 M NaCl (pH 9.5) overnight. FITC was dissolved (1 mg/ml) in 0.1 M Na_2CO_3 (pH 9.5) and was added to the endostatin, Aβ or hIAPP solutions at 2 μg FITC/mg protein. After a 4 h incubation at room temperature free FITC molecules were removed by dialysis against 1 M Tris, pH 7.5, and subsequently, against PBS. During this procedure endostatin stays soluble and becomes highly fluorescent. Aggregated FITC-labeled endostatin was prepared from soluble FITC-labeled endostatin as above. Freshly solubilized as well as pre-aggregated Aβ and hIAPP were labeled with FITC by the same protocol. Cells grown on glass coverslips were exposed to FITC-labeled soluble or aggregated endostatin (5 μM), freshly resuspended or pre-aggregated Aβ or hIAPP for 6 h and were subsequently washed five times in PBS to discard unbound material. The coverslips were then fixed by addition of formaldehyde (3.7% in PBS). Following fixation, the cells were incubated for 30 min in PBS–BSA (bovine serum albumin; 0.1%) containing Texas red-conjugated phalloidin to stain the actin cytoskeleton. The coverslips were then washed twice with PBS and were subsequently mounted in Vectashield containing DAPI (to stain cell nuclei) and analyzed using a Leica DM-IRBE fluorescence microscope. Quantitation of aggregate binding to cells was performed as follows: 10 random fields were selected in a blind manner (i.e. without knowledge of the coverslips' identity) in the red channel (actin). Images were subsequently automatically taken in all three channels by using Qfluoro software. The images were then analyzed by assessing the number of FITC-labeled aggregates per field by using Leica Qwin software. Alternatively, the samples were analyzed by confocal microscopy (Leica) and images were processed using Leica software.

2.10. Analysis of cell death

After exposure to endostatin or Aβ (25 μM, 24 h) cells in the culture medium were collected and the remaining adherent cells were trypsinized and added to the detached cells in the medium, thus obtaining the total pool of adherent and detached cells. Subsequently, the cells were stained with 0.02% Trypan blue and the percentage dead (Trypan blue-positive) cells was assessed using a Bürker glass counter chamber. Triplicate samples were analyzed and 200 cells were counted in each sample.

2.11. Annexin V labeling

Cells were grown on glass coverslips and, following exposure to either soluble or aggregated (non-fluorescent) endostatin or Aβ (25 μM, 24 h), were fixed in the culture medium using 3.7% formaldehyde. Subsequently, the cells were analyzed for the presence of exposed phosphatidyl-serine on the cell surface using FITC-labeled annexin V (Sigma) according to the manufacturer's protocol.

3. Results and discussion

3.1. Bacterial endostatin forms amyloid fibers with cross-β structure

In solution, properly folded proteins or peptides form a stable three-dimensional structure. However, protein fragments (like endostatin) are often prone to (partial) denaturation. As a result, they may aggregate and become insoluble. Insoluble proteins may either exist as amorphous aggregates or as highly ordered amyloid deposits [18]. The latter structure results from extensive 'cross-β sheet' formation [19]. In cross-β sheets the polypeptide backbones are in a β-sheet conformation with hydrogen bonds between the separate polypeptide backbones. Congo red is a dye that is used for the detection of cross-β sheet-forming amyloid deposits, showing green birefringence under polarized light [20]. We found that insoluble endostatin, as it is produced from bacteria, binds Congo red (Fig. 1A). Furthermore, when examined under polarized light it exhibits the green birefringence that is characteristic for Congo red-bound amyloid deposits.

Next, we investigated whether cross-β sheets are indeed present in bacterial endostatin by performing X-ray diffraction analysis [21]. We found that the bacterial endostatin sample produced distinct reflection lines at 4.7 Å (hydrogen-bond distance), as well as at 10–11 Å (inter-sheet distance) (Fig. 1B). It is important to note that the reflection lines at 4.7 Å and 10–11 Å show maximal intensities at opposite diffraction angles (Fig. 1B). The fiber axis with its 4.7 Å hydrogen-bond repeat distance is oriented along the vertical capillary axis. This implies that the inter-sheet distance of 10–11 Å is perpendicular to these hydrogen bonds in the protein aggregates. This is consistent with the protein being in a cross-β sheet conformation (see also [22]). Intramolecular β-sheets in a globular protein cannot cause a diffraction pattern that is so ordered. A rough estimate of 54 Å for the crystallite size in the hydrogen-bond direction is obtained from the width of the 4.7 Å reflection. This corresponds to about 11–12 β strands connected by hydrogen bonds. The scattering of the 10–11 Å

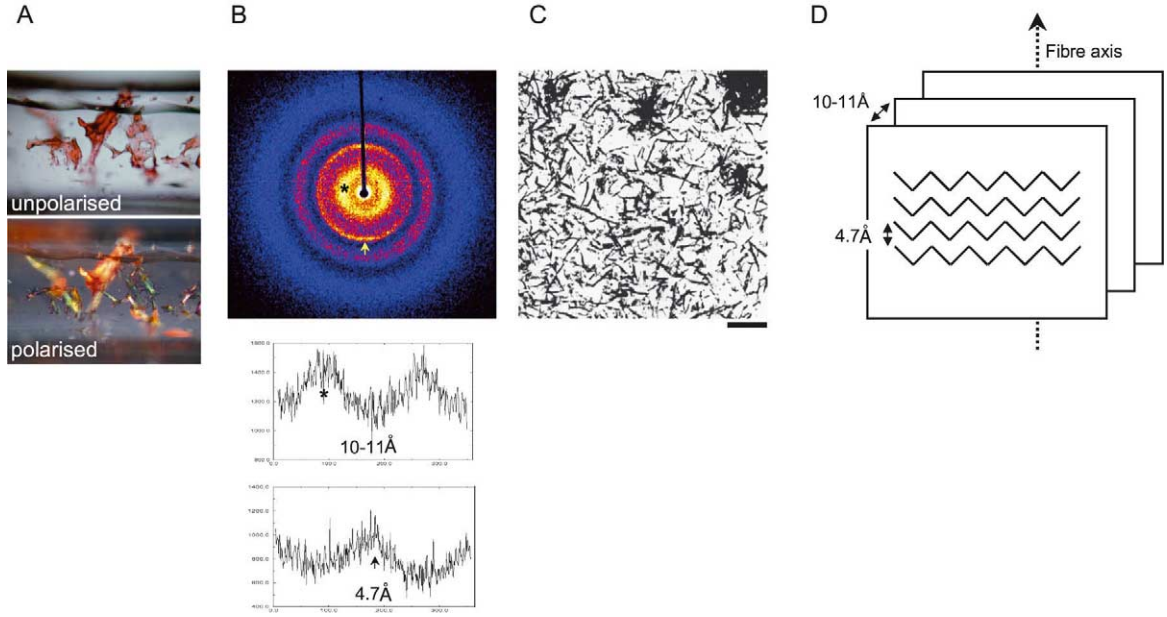

Fig. 1. Amyloid properties of endostatin produced in bacteria. A: Endostatin was purified from bacteria. The resulting aggregates were partially dissolved in 0.1% formic acid, taken up in a glass capillary and were stained with Congo red. Samples were then analyzed by light microscopy using both polarized and non-polarized light. The figure shows that endostatin binds Congo red and exhibits green birefringence when examined under polarized light. B: Endostatin samples were prepared as in panel A and were subsequently analyzed by X-ray diffraction. The scattering as obtained on the 2D detector is color-coded by intensity on a linear scale. The scattering intensity decreases as white–yellow–red–blue–black. The pattern shows diffraction maxima at 4.7 and 10–11 Å. The fiber axis (hydrogen-bond direction) with 4.7 Å repeat is oriented vertically and is indicated by the arrow. The 10–11 Å repeat is preferentially oriented perpendicular to that, as indicated by the asterisk. Tangential scans along the 2θ scattering angles corresponding to both d spacings in the lower panel show that the scattering at 4.7 Å is oriented vertically and that at 10–11 Å horizontally. C: Endostatin samples were prepared as in A, but were coated on a 400 mesh grid and were processed for TEM. Endostatin forms fibrils with a diameter of ~30 nm and lengths ranging from 150 to 500 nm. D: Model of the endostatin fiber. The measured distances between individual peptide backbones (H-bonds) and between the distinct sheets are indicated, as well as the fiber axis (see also [17]). A rough estimate of 54 Å for the crystallite size along the fiber axis corresponds to about 11–12 β strands connected by hydrogen bonds.

repeat is broad as usual. This is due both to the limited crystallite size in the inter-sheet direction and to variation in the inter-sheet distance. From the amount of background scattering it follows that only part of the protein is involved in cross-β sheet formation.

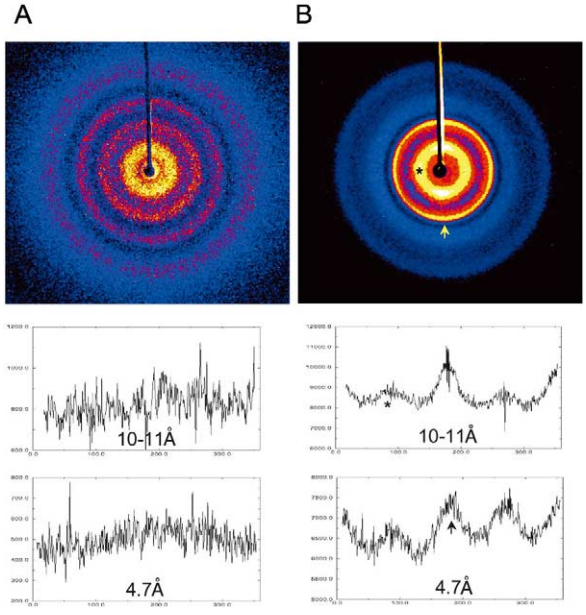

Proteins and peptides that form cross-β sheets have the tendency to aggregate into fibrillar structures that can be visualized by TEM [23]. Therefore, we examined the endostatin aggregates using TEM. Fig. 1C shows that bacterial endostatin forms unbranched fibers with a diameter of approximately 300 Å (30 nm) and with lengths varying from 1500 to 5000 Å (15–500 nm). Characteristic amyloid peptides form fibrils with diameters ranging from 50 to 130 Å (5–13 nm) [18] and with varying lengths up to 1 μm. Taken together, our results show that bacterial endostatin is a protein fragment with an inherent propensity to form cross-β sheets and to aggregate into relatively thick amyloid-like fibrils.

←

Fig. 2. Conversion of soluble globular endostatin into amyloid endostatin. Endostatin produced in yeast was dialyzed against 8 M urea followed by extensive dialysis against H_2O. During dialysis endostatin precipitates as a fine white solid. Formic acid (0.1%) was added to both untreated and urea-treated endostatin preparations as in Fig. 1A. The samples were subsequently processed for X-ray diffraction analysis. A: Diffraction pattern of untreated (yeast-produced) endostatin with no sign of cross-β sheet structure. B: Diffraction pattern of urea-treated endostatin with extensive cross-β sheet formation. During solvent evaporation fibril formation occurred both vertically and horizontally in the capillary, as evidenced by the occurrence of peaks at 90°, 180°, 270° and 0°/360° in the tangential scans corresponding to both d spacings. The asterisk indicates the peak reflection of the 10–11 Å d spacing at 90°. The arrow indicates the peak reflection of the 4.7 Å d spacing at 180°.

3.2. Conversion of soluble yeast-produced endostatin into amyloid endostatin

In contrast to bacterial endostatin, endostatin produced in yeast is soluble, and neither binds Congo red, nor forms amyloid fibrils when examined using TEM (data not shown). A major difference in the isolation protocols is a denaturation step using 8 M urea during the isolation of endostatin from bacteria, but not from yeast. Since amyloid formation occurs via (partially) denatured intermediates [18], we considered the possibility that this step may allow for the efficient stacking of endostatin monomers to form cross-β sheets. Therefore, we subjected soluble yeast endostatin to the same denaturation/renaturation protocol and examined the resulting preparation for cross-β sheet content using X-ray diffraction. Fig. 2A shows that soluble endostatin produced in yeast does not show any signs of cross-β sheet formation. The diffraction pattern is typical for any amorphous globular protein and does not show a sharp reflection line at 4.7 Å. Furthermore, there is no perpendicular orientation of the diffuse reflection lines at 4.7 Å and 9–11 Å. The X-ray diffraction data are in line with our findings that soluble endostatin does not bind to Congo red and does not form fibrils. However, after denaturation/renaturation we found extensive cross-β sheet formation in yeast-produced endostatin (Fig. 2B). In addition to urea treatment, protein denaturation through freeze–thawing or heating also induced endostatin aggregation (data not shown). We conclude that endostatin is a protein with a high propensity to form amyloid aggregates, a process that is greatly enhanced when the protein undergoes (partial) denaturation. In this light it is interesting to note that the β-sheet content measured in the endostatin crystal (25%) does not match the percentage of β-sheet content of the original solution (70%) [17,24]. This implies that the solution from which the crystal has grown contained a β-sheet-rich form(s) of endostatin that did not crystallize. Due to the intrinsic heterogeneity of cross-β sheet forming proteins, crystallization of such structures is notoriously difficult.

3.3. Binding of endostatin to N1E-115 cells requires cross-β structure

The prototype amyloid protein is Aβ, a 40–42 amino acid peptide that is found as insoluble aggregates in neuronal tissue and in the brain microvasculature of Alzheimer's disease patients [25]. Like endostatin and many other amyloid proteins or peptides, Aβ is a naturally occurring cleavage product of a larger precursor protein [25]. In vitro, Aβ has toxic effects on both endothelial and neuronal cell types [26–31].

Based on the observed structural similarities between endostatin and Aβ we investigated whether endostatin would bind to and be toxic to neuronal cells. To this end we used the N1E-115 murine neuroblastoma cell line that can differentiate into post-mitotic neurons in vitro [32]. First, we tested whether endostatin can bind to these cells. Soluble endostatin was labeled with FITC and was either left untreated or was treated to form amyloid aggregates as above. As controls we also used FITC-labeled Aβ and hIAPP. The latter peptides were used in two structural conformations: freshly resuspended (non-cross-β) and pre-aggregated (cross-β). Cells

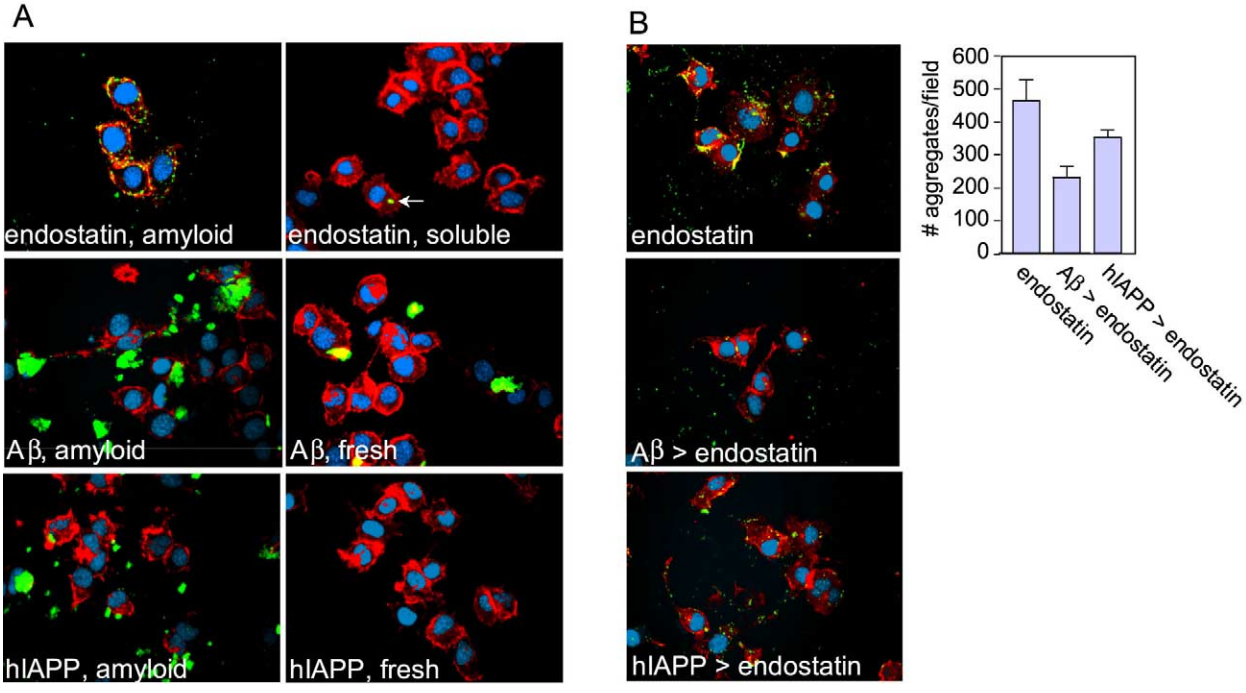

Fig. 3. Binding of amyloid aggregates to N1E-115 neuroblastoma cells. A: Neuronal N1E-115 cells, grown on glass coverslips, were incubated for 1 h with either FITC-labeled aggregated amyloid endostatin, soluble endostatin, Aβ freshly resuspended, Aβ pre-aggregated for 3 weeks (Aβ amyloid), hIAPP freshly resuspended and hIAPP pre-aggregated for 3 weeks (hIAPP amyloid) (all at 5 μM). Cells were subsequently extensively washed and fixed. The actin cytoskeleton was stained using Texas red-conjugated palloidin (red) and the DNA with DAPI (blue). The coverslips were then analyzed by conventional fluorescence microscopy. Shown are merged images. All amyloid aggregates (left panels) bound N1E-115 cells. B: N1E-115 cells were pre-incubated for 6 h with non-fluorescent Aβ or hIAPP (at 5 μM) and the binding of FITC-labeled amyloid endostatin (1 h, 5 μM) was subsequently tested as above. Digital image analysis shows that pre-incubation of the cells with Aβ and, to a lesser extent, hIAPP diminishes endostatin binding (to 50% and 25%, respectively), suggesting that the aggregates have common cellular binding sites. The bar diagram shows means of 10 randomly selected fields in the red channel to avoid bias.

were exposed to soluble or aggregated endostatin, to Aβ or to hIAPP for 1 h. Following extensive washing and fixation, binding of endostatin, Aβ and hIAPP to the cells was assessed by fluorescence microscopy. Fig. 3A shows that soluble endostatin is found neither associated to the cells, nor inside the cells, nor on the matrix surrounding the cells. In contrast, the majority of amyloid endostatin is cell-associated. Some of the deposits localized to the matrix, and some were found inside the cells (see below). Like amyloid endostatin, both Aβ and hIAPP readily bound to the cells. Two distinct types of aggregates were observed: small endostatin-like aggregates as well as larger aggregates that are not observed in the endostatin preparation. In the freshly resuspended (non-cross-β) peptides the small aggregates were not observed but larger aggregates were occasionally found to be cell-associated (Fig. 3). It is well known that the formation of extensive cross-β structure in these peptide aggregates may take days to weeks.

When using high concentrations of soluble endostatin, we observed occasional protein aggregation in the tissue culture medium and these aggregates were found to bind to the cells (Fig. 3 upper panel, arrow). This indicates once again the propensity of soluble endostatin to undergo structural changes leading to amyloid aggregation. Factors present in the medium or in the serum may promote this conversion.

We reasoned that if cross-β structure underlies the binding of aggregated endostatin to the cells, amyloid β and hIAPP may compete for endostatin binding. We tested this by incubating the cells for 6 h with either Aβ or with hIAPP prior to incubation with amyloid endostatin for 1 h. The binding of endostatin to the cells was then assessed by fluorescence microscopy and subsequent digital image analysis. Fig. 3B shows that Aβ and, to a lesser extent, hIAPP compete with amyloid endostatin for binding to the N1E-115 cells. Thus, amyloid endostatin shares cellular binding sites with other amyloid peptides, even though these peptides and endostatin do not share any overt primary sequence homology. We next extended these observations by analyzing the binding of endostatin, Aβ and hIAPP to N1E-115 cells in more detail. To this end we allowed binding of the FITC-labeled aggregates to the cells as above and, following extensive washing and staining of the actin acytoskeleton with Texas red phalloidin, the cell-bound aggregates were examined by confocal microscopy. Fig. 4 shows images of single cells and of highly zoomed fragments of the cell surface in which discrete single aggregates are visible. We found that the majority of all three amyloid aggregates are in close proximity to the cortical actin-cytoskeleton that is connected to the plasma membrane (Fig. 4). In addition, some of the aggregates are found inside the cells (arrows), indicating that at least some internalization of the aggregates can take place.

3.4. *Amyloid but not soluble endostatin is cytotoxic to N1E-115 neuroblastoma cells*

Next, we analyzed whether the distinct forms of endostatin would be cytotoxic to differentiated N1E-115 cells and compared their cytotoxicity with that induced by Aβ. Fig. 5A shows that amyloid but not soluble endostatin binds to differentiated N1E-115 cells as it does to the undifferentiated cells (Figs. 3 and 4). Furthermore, we found that a 24 h exposure of these cells to either Aβ or to amyloid endostatin induced cell death, whereas soluble endostatin or buffer controls had no effect on neuronal cell viability (Fig. 5). Amyloid peptides may induce either apoptosis or necrosis in neuronal and endothelial cells. Annexin V strongly binds to exposed phosphatidyl-serine, a marker for apoptotic cell death. We found that cells treated with amyloid endostatin, but not those treated with soluble endostatin, are highly positive for fluorescent annexin V (Fig. 5C), indicating that endostatin-induced cell death is apoptotic in nature.

Interestingly, a recent report showed the production of endostatin by neuronal cells and the localization of endostatin to Aβ plaques in Alzheimer's disease brain [33]. However, the structural basis of this interaction was not examined. Given our finding that endostatin, like Aβ, has the propensity to form cross-β structure, a cross-β type interaction may account

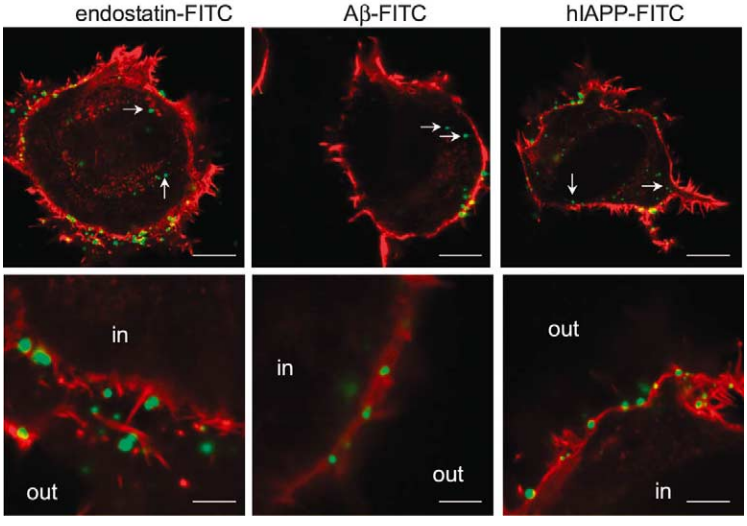

Fig. 4. Localization of cell-associated amyloid aggregates. N1E-115 cells were grown on glass coverslips and were incubated for 1 h with FITC-labeled amyloid endostatin, Aβ and hIAPP. Actin was visualized using Texas red-conjugated phalloidin. The coverslips were analyzed by confocal microscopy. Whole cell images (upper panel) show localization of all three amyloids mainly to the cell surface. In addition, some of the aggregates show intracellular localization (arrows) (bar, 10 μm). Zoomed images of cell surface areas (lower panel) show that all three types of amyloid aggregates are in close proximity to the plasma membrane-bound cortical actin cytoskeleton (bar, 2 μm).

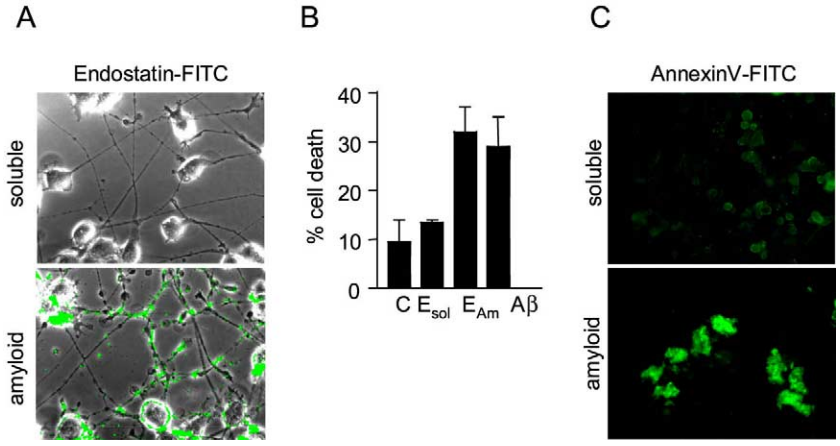

Fig. 5. Toxicity of amyloid endostatin. A: N1E-115 cells were differentiated into post-mitotic neurons on glass coverslips and were subsequently treated overnight with either FITC-labeled soluble or with FITC-labeled amyloid endostatin. Following extensive washing and fixation, binding of endostatin to the cells was visualized with fluorescence microscopy. Merged bright field and fluorescence images are shown. Only amyloid endostatin binds to the differentiated neuronal cells. B: Differentiated N1E-115 cells were treated for 24 h with either buffer, soluble endostatin (25 μM) (Esol), amyloid endostatin (25 μM) (EAm), or with Aβ (25 μM). Cell viability was subsequently assessed by Trypan blue exclusion, counting both adherent and detached cells. The bar diagram shows means of triplicate samples. C: N1E-115 cells were differentiated on glass coverslips and were subsequently treated with either soluble or amyloid endostatin. Following fixation, the cells were stained with annexin V-FITC to visualize exposed phosphatidyl-serine. Detaching cell clusters that are associated with endostatin aggregates are highly positive for annexin V.

for their co-localization in vivo. Taken together, it seems likely that endostatin may affect neuronal cell function and survival, also in vivo.

In addition to using neuronal N1E-115 cells we also used bovine pulmonary aortic endothelial cells. We found that amyloid endostatin, but not soluble endostatin, is highly cytotoxic to these cells as it is to the neuronal cells. In contrast, neither soluble nor amyloid endostatin was cytotoxic to primary human umbilical vein endothelial cells nor to human dermal microvascular endothelial cells (data not shown). At present we do not know what determines the sensitivity of (endothelial or neuronal) cells to amyloid endostatin. Possibly, amyloid endostatin may exert its toxic effects by activating amyloid receptors on the cell surface like receptor for advanced glycation end products or scavenger receptors like CD36 [34,35].

Can amyloid toxicity explain the anti-angiogenic effect of endostatin? We found the formation of liver metastases by C26 murine colon cancer cells to be sensitive to treatment with endostatin. In this model both soluble and amyloid endostatin inhibited tumor growth, but neither form caused tumor regression [36] (and te Velde et al., submitted). Given the propensity of soluble endostatin to aggregate and the inability to control this phenomenon in vivo, it is impossible to assign anti-tumor activity to a specific structural form of endostatin.

4. Concluding remarks

Although many reports have shown effects of either soluble or insoluble endostatin on cell behavior [3], it is far from clear which mechanisms underlie which phenomena. Induction of apoptosis and inhibition of cell migration seem to be the most commonly found cellular effects [3]. Our results provide an explanation for the observed cytotoxic effects of endostatin. Amyloid formation often occurs in protein fragments that are taken out of their natural context (i.e. the full-length protein), presumably due to partial denaturation [18]. The hydrophobicity of the peptide sequence and the propensity of the sequence to form β-sheets are critical determinants of protein aggregation [37]. Recently it was found that two unrelated protein fragments (which, unlike Aβ, are not related to any disease) become highly toxic upon aggregation [38]. Taken together, it seems likely that protein aggregation per se, independent of the primary amino acid sequence, endows aggregated amyloid proteins with an inherent toxicity [38]. The results presented here suggest that endostatin can be added to the list of 'toxic-when-aggregated' proteins. It is to be expected that this list will become much longer in the near future. It is important to note that the extent of toxicity is determined largely by the level of aggregation and the structural basis of aggregation [38]. These phenomena, in turn, greatly depend on a number of parameters, including protein production and storage protocols, pH, and choice of solvents.

Our results show that endostatin-induced cytotoxicity is restricted to the aggregated amyloid form. Endostatin is toxic to endothelial [7–9] and neuronal (this study) cells. These cell types are also particularly sensitive to amyloid deposits [26–31]. Our finding that endostatin is a protein with amyloid properties may therefore explain the cell-type specificity of its cytotoxicity. If endostatin exerts its effect through cellular receptors, its bioactivity will depend on the expression of such receptors on the target cells. Therefore, we are presently studying whether endostatin can activate receptors that are known to bind to cross-β sheet peptides.

Acknowledgements: We thank Laurent Mosnier, Joost Meijers and Bonno Bouma for stimulating discussions. This work was sponsored in part by the Dutch Cancer Society and by Crucell N.V., Leiden, The Netherlands.

References

[1] Cao, Y. (2001) Int. J. Biochem. Cell Biol. 33, 357–369.
[2] Los, M. and Voest, E.E. (2001) Semin. Oncol. 28, 93–105.
[3] Sim, B.K., MacDonald, N.J. and Gubish, E.R. (2000) Cancer Metastasis Rev. 19, 181–190.
[4] Zogakis, T.G. and Libutti, S.K. (2001) Expert. Opin. Biol. Ther. 1, 253–275.

[5] O'Reilly, M.S., Boehm, T., Shing, Y., Fukai, N., Vasios, G., Lane, W.S., Flynn, E., Birkhead, J.R., Olsen, B.R. and Folkman, J. (1997) Cell 88, 277–285.
[6] Boehm, T., Folkman, J., Browder, T. and O'Reilly, M.S. (1997) Nature 390, 404–407.
[7] Dhanabal, M., Ramchandran, R., Waterman, M.J., Lu, H., Knebelmann, B., Segal, M. and Sukhatme, V.P. (1999) J. Biol. Chem. 274, 11721–11726.
[8] Dhanabal, M., Volk, R., Ramchandran, R., Simons, M. and Sukhatme, V.P. (1999) Biochem. Biophys. Res. Commun. 258, 345–352.
[9] Dixelius, J., Larsson, H., Sasaki, T., Holmqvist, K., Lu, L., Engstrom, A., Timpl, R., Welsh, M. and Claesson-Welsh, L. (2000) Blood 95, 3403–3411.
[10] Ackley, B.D., Crew, J.R., Elamaa, H., Pihlajaniemi, T., Kuo, C.J. and Kramer, J.M. (2001) J. Cell Biol. 19, 1219–1232.
[11] Yamaguchi, N., Anand-Apte, B., Lee, M., Sasaki, T., Fukai, N., Shapiro, R., Que, I., Lowik, C., Timpl, R. and Olsen, B.R. (1999) EMBO J. 18, 4414–4423.
[12] Eisterer, W., Jiang, X., Bachelot, T., Pawliuk, R., Abramovich, C., Leboulch, P., Hogge, D. and Eaves, C. (2002) Mol. Ther. 5, 352–359.
[13] Jouanneau, E., Alberti, L., Nejjari, M., Treilleux, I., Vilgrain, I., Duc, A., Combaret, V., Favrot, M., Leboulch, P. and Bachelot, T. (2001) J. Neurooncol. 51, 11–18.
[14] Marshall, M. (2002) Science 295, 2198–2199.
[15] Pawliuk, R., Bachelot, T., Zurkiya, O., Eriksson, A., Cao, Y. and Leboulch, P. (2002) Mol. Ther. 5, 345–351.
[16] Ding, Y.H., Javaherian, K., Lo, K.M., Chopra, R., Boehm, T., Lanciotti, J., Harris, B.A., Li, Y., Shapiro, R., Hohenester, E., Timpl, R., Folkman, J. and Wiley, D.C. (1998) Proc. Natl. Acad. Sci. USA 95, 10443–10448.
[17] Hohenester, E., Sasaki, T., Olsen, B.R. and Timpl, R. (1998) EMBO J. 17, 1656–1664.
[18] Rochet, J.C. and Lansbury Jr., P.T. (2000) Curr. Opin. Struct. Biol. 10, 60–68.
[19] Lansbury Jr., P.T. (1992) Biochemistry 31, 6865–6870.
[20] Elghetany, M.T. and Saleem, A. (1988) Stain Technol. 63, 201–212.
[21] Serpell, L.C., Fraser, P.E. and Sunde, M. (1999) Methods Enzymol. 309, 526–536.
[22] Kranenburg, O., Bouma, B., Kroon-Batenburg, L.M., Reijerkerk, A., Wu, Y.P., Voest, E.E. and Gebbink, M.F.B.G. (2002) Curr. Biol. 12, 1833–1839.
[23] Balbach, J.J., Ishii, Y., Antzutkin, O.N., Leapman, R.D., Rizzo, N.W., Dyda, F., Reed, J. and Tycko, R. (2000) Biochemistry 39, 13748–13759.
[24] Sasaki, T., Fukai, N., Mann, K., Gohring, W., Olsen, B.R. and Timpl, R. (1998) EMBO J. 17, 4249–4256.
[25] Selkoe, D.J. (2001) Physiol. Rev. 81, 741–766.
[26] Blanc, E.M., Toborek, M., Mark, R.J., Hennig, B. and Mattson, M.P. (1997) J. Neurochem. 68, 1870–1881.
[27] Koh, J.Y., Yang, L.L. and Cotman, C.W. (1990) Brain Res. 19;533, 315–320.
[28] Pike, C.J., Burdick, D., Walencewicz, A.J., Glabe, C.G. and Cotman, C.W. (1993) J. Neurosci. 13, 1676–1687.
[29] Simmons, L.K., May, P.C., Tomaselli, K.J., Rydel, R.E., Fuson, K.S., Brigham, E.F., Wright, S., Lieberburg, I., Becker, G.W. and Brems, D.N. (1994) Mol. Pharmacol. 45, 373–379.
[30] Suo, Z., Fang, C., Crawford, F. and Mullan, M. (1997) Brain Res. 762, 144–152.
[31] Yankner, B.A., Duffy, L.K. and Kirschner, D.A. (1990) Science 250, 279–282.
[32] Kranenburg, O., Scharnhorst, V., Van der Eb, A.J. and Zantema, A. (1995) J. Cell Biol. 131, 227–234.
[33] Deininger, M.H., Fimmen, B.A., Thal, D.R., Schluesener, H.J. and Meyermann, R. (2002) J. Neurosci. 22, 10621–10626.
[34] Husemann, J., Loike, J.D., Anankov, R., Febbraio, M. and Silverstein, S.C. (2002) Glia 40, 195–205.
[35] Stern, D., Du, Y.S., Fang, Y.S. and Marie, S.A. (2002) Adv. Drug Deliv. Rev. 54, 1615–1625.
[36] te Velde, E.A., Vogten, J.M., Gebbink, M.F.B.G., van Gorp, J.M., Voest, E.E. and Borel Rinkes, I.H.M. (2002) Br. J. Surg. 89, 1302–1309.
[37] Chiti, F., Taddei, N., Baroni, F., Capanni, C., Stefani, M., Ramponi, G. and Dobson, C.M. (2002) Nat. Struct. Biol. 9, 137–143.
[38] Bucciantini, M., Giannoni, E., Chiti, F., Baroni, F., Formigli, L., Zurdo, J., Taddei, N., Ramponi, G., Dobson, C.M. and Stefani, M. (2002) Nature 416, 507–511.